Magnetic Breakdown in the Electron-Doped Cuprate Superconductor $Nd_{2-x}Ce_xCuO_4$: The Reconstructed Fermi Surface Survives in the Strongly Overdoped Regime

T. Helm,[1] M. V. Kartsovnik,[1,*] I. Sheikin,[2] M. Bartkowiak,[3] F. Wolff-Fabris,[3] N. Bittner,[1] W. Biberacher,[1]
M. Lambacher,[1] A. Erb,[1] J. Wosnitza,[3] and R. Gross[1,4]

[1]*Walther-Meißner-Institut, Bayerische Akademie der Wissenschaften, Walther-Meißner-Straße 8, D-85748 Garching, Germany*
[2]*Laboratoire National des Champs Magnétiques Intenses, CNRS, 25 rue des Martyrs B.P. 166, 38042 Grenoble Cedex 9, France*
[3]*Hochfeld-Magnetlabor Dresden, Forschungszentrum Dresden-Rossendorf, Bautzner Landstraße 400, D-01328 Dresden, Germany*
[4]*Physik-Department, Technische Universität München, James Franck Straße, D-85748 Garching, Germany*
(Received 13 August 2010; published 9 December 2010)

We report on semiclassical angle-dependent magnetoresistance oscillations and the Shubnikov–de Haas effect in the electron-overdoped cuprate superconductor $Nd_{2-x}Ce_xCuO_4$. Our data provide convincing evidence for magnetic breakdown in the system. This shows that a reconstructed multiply connected Fermi surface persists, at least at strong magnetic fields, up to the highest doping level of the superconducting regime.

The recent discovery of magnetic quantum oscillations in the resistivity of hole- [1–4] and electron-doped [5] cuprate superconductors clearly demonstrates the importance of high-field magnetotransport experiments for exploring the Fermi surface in these materials. In particular, quantum oscillations of the magnetoresistance, the Shubnikov–de Haas (SdH) effect, observed in the electron-doped cuprate $Nd_{2-x}Ce_xCuO_4$ (NCCO) have proved to be very useful for tracing changes in the Fermi surface with varying carrier concentration [5]. For $x = 0.17$, corresponding to nearly the border of the superconducting regime on the overdoped side, high-frequency SdH oscillations were found which are in perfect agreement with the large cylindrical Fermi surface predicted by band structure calculations [6] and angle-resolved photoemission spectroscopy (ARPES) [7,8]. However, lowering the Ce concentration by just 1% leads to their suppression and the emergence of much slower oscillations [5]. The slow oscillations observed for optimally doped ($x = 0.15$) and slightly overdoped ($x = 0.16$) NCCO crystals indicate that the Fermi surface is reconstructed in this doping range, at least at high magnetic fields. It is, thus, tempting to suggest a quantum phase transition associated with a translational symmetry breaking at a doping level between $x = 0.16$ and 0.17. This is supported by in-plane magnetotransport data at lower magnetic fields on another electron-doped superconductor $Pr_{2-x}Ce_xCuO_4$ [9] implying a quantum critical point at $x \approx 0.165$. However, a similar experiment on NCCO [10] rather indicates two small groups of carriers and, hence, a reconstructed Fermi surface persisting up to $x = 0.17$. Moreover, it was pointed out [5,11] that the observation of fast SdH oscillations does not unambiguously rule out the Fermi surface reconstruction for $x = 0.17$: if the potential responsible for the symmetry breaking is nonzero but weak, such oscillations can arise as a result of magnetic breakdown. Thus, the question of

whether the quantum phase transition occurs inside the superconducting doping range or the reconstructed Fermi surface survives throughout the entire superconducting dome is still open and one of the key issues in high temperature superconductivity.

Another important question is related to the exact shape of the reconstructed Fermi surface in overdoped NCCO. It was proposed [5,11] that the reconstruction occurs due to a $(\pi/a, \pi/a)$ density wave ordering (a is the lattice constant in the CuO_2 plane). Indeed, the measured frequency of the slow SdH oscillations is consistent with the size of small hole pockets, which should be formed around $(\pi/2a, \pi/2a)$ due to such ordering. However, to verify this scenario it is desirable to determine not only the size but also the shape of the Fermi pockets. Towards this end, a very efficient method which has been widely used for mapping the in-plane Fermi surfaces of organic conductors [12] and other layered systems such as Sr_2RuO_4 [13] and intercalated graphite [14] is semiclassical angle-dependent magnetoresistance oscillations (AMRO). This is a geometric effect directly related to the shape of a weakly warped cylindrical Fermi surface [15–18]. It has also been observed in hole-overdoped $Tl_2Ba_2CuO_{6+\delta}$ (Tl2201) [17,19] and used to extract the shape of the Fermi surface both within the plane of the conducting layers and in the out-of-plane direction, as well as to evaluate the scattering anisotropy. However, Tl2201 is the only member of the cuprate family in which AMRO have been found so far.

Here, we report on the interlayer resistivity of overdoped NCCO studied as a function of the orientation and strength of the applied magnetic field. We present angle-dependent magnetoresistance patterns for crystals with $x = 0.16$ and 0.17 which exhibit distinct features characteristic of AMRO. Most remarkably, for both doping levels the AMRO positions are found to be very similar. Together with the earlier SdH data [5], this result implies magnetic

breakdown in the system. This conclusion is confirmed by a new high-resolution SdH experiment on strongly overdoped ($x = 0.17$) NCCO which clearly reveals the presence of a weak superlattice potential up to the highest doping level.

The NCCO crystals used in our experiments were grown by traveling solvent floating zone technique and characterized as described elsewhere [20]. For the measurements of the angle-dependent magnetoresistance, the samples were mounted on a two-axes rotating stage allowing *in situ* rotations at low temperatures, at a fixed magnetic field up to 28 T generated by the 20 MW resistive magnet at the Grenoble High Magnetic Field Laboratory. The interlayer resistance was measured as a function of polar angle θ between the field direction and crystallographic [001] axis of the sample, at different fixed azimuthal angles φ, as shown in Fig. 1(a). The SdH experiment was done at the Hochfeld-Magnetlabor Dresden in pulsed fields up to 65 T applied perpendicular to CuO$_2$ layers.

Figures 1(b) and 1(d) show the angle-dependent interlayer resistivity ρ_c of NCCO with $x = 0.16$ and 0.17, respectively, recorded at different temperatures for $\varphi = 45°$ and $B = 28$ T. At this field, superconductivity at low temperatures is manifest by a sharp dip within a narrow angular range around $\pm 90°$. In the normal state, we

FIG. 1 (color online). (a) Sketch of the experimental configuration. (b) Interlayer resistivity ρ_c of a slightly overdoped NCCO sample ($x = 0.16$) as a function of tilt angle θ, at different temperatures. The range $|\theta| < 75°$ corresponds to the normal conducting state; the rapid drop of ρ_c outside this range is due to onset of superconductivity. The vertical dashed lines are drawn through the AMRO features centered at $|\theta| \approx 53°$, which are independent of temperature and magnetic field strength. (c) Second derivative of the resistivity in (b) exhibiting dips at the AMRO peak positions. (d) Same as (b) for a strongly overdoped sample ($x = 0.17$).

observe a prominent maximum at $\theta = 0°$ and, in addition, a pair of shallow humps superimposed on the monotonic slope around $\theta \approx \pm 53°$. To illustrate them more clearly, Fig. 1(c) shows the second derivative $d^2\rho_c/d\theta^2$ exhibiting dips at these angles. These features, though rather weak, were reproduced for several samples at both doping levels. To the accuracy of the experiment, the angular positions of the features are independent of temperature; see Fig. 1. We have also checked that they do not shift on reducing the field strength down to 23 T. This is exactly what one expects for AMRO, whose positions are solely determined by the Fermi surface geometry.

For $T \leq 10$ K, the magnetoresistance behavior shown in Fig. 1 resembles that observed earlier on hole-overdoped Tl2201 [17,19]. For the latter compound, it was shown that both the central hump and the side features originated from the AMRO effect on the large cylindrical Fermi surface. In particular, the resistivity peak at $\theta = 0°$ was considered as a fingerprint of a warped Fermi cylinder centered at the corner of the Brillouin zone and satisfying the symmetry requirements of a body-centered tetragonal lattice [17]. Since NCCO has the same crystal symmetry, it is tempting to also attribute the central hump in our $\rho_c(\theta)$ curves to the large Fermi cylinder. We note, however, that unlike at $\theta \approx \pm 53°$, the field direction corresponding to $\theta = 0°$ coincides with the crystal symmetry axis normal to the layers, which should always lead to an extremum in the $\rho_c(\theta)$ dependence. Therefore, one should not disregard other possible mechanisms, besides AMRO, which could cause a maximum at this field direction. Indeed, the experimentally observed evolution of the central hump with temperature is opposite to that expected for AMRO. Since AMRO are an effect of the cyclotron motion of charge carriers in a strong magnetic field, they require a sufficiently large scattering time τ. As τ decreases with increasing T, the AMRO are expected to gradually vanish. This is, indeed, the case for the humplike features around $\theta \approx \pm 53°$ in Fig. 1 which can hardly be resolved above 20 K. By contrast, the central hump notably increases in magnitude, dominating the angular dependence at elevated temperatures. In fact, the overall shape of the 23 K curve for $x = 0.16$ and 50 K curve for $x = 0.17$ in Fig. 1, exhibiting a global maximum at **B** normal to the layers and parallel to the current direction, is at odds with the usual orbital effect of a magnetic field on the coherent interlayer charge transport. While the exact mechanism responsible for this anomalous behavior has still to be established, it is clear that, at least at high T, the central hump cannot be attributed to the AMRO. As the scattering time increases at cooling down below 20 K, the conventional orbital effect becomes significant, which is evidenced by the development of the positive slope $d\rho_c/d|\theta|$ at $|\theta| \geq 30°$ and the AMRO features at $|\theta| \approx 53°$. It is also possible that the central hump is partly due to the AMRO at low temperatures. However, further studies are needed to clarify this.
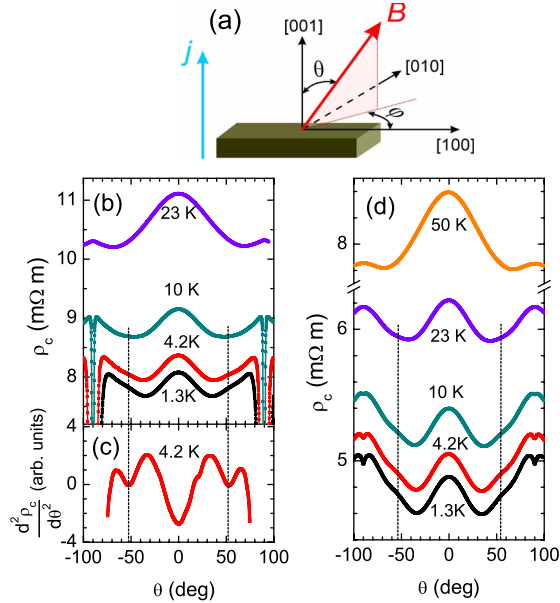
The weakness of the AMRO features indicates that even at 28 T the high-field criterion, $\omega_c \tau \gg 1$ (ω_c is the characteristic cyclotron frequency), is by far not fulfilled. In this situation, simple Yamaji-like conditions for the AMRO positions [12,15,16] are not applicable and a detailed quantitative analysis of the angle-dependent magnetoresistance is required for the determination of the relevant Fermi surface geometry [17–19]. This is, however, problematic in the present case due to the above mentioned coexistence of an anomalous and conventional orbital magnetotransport mechanisms. Further experiments in an extended field and temperature range, at different doping levels, are required for separating these two contributions. Although a detailed quantitative analysis is out of reach, very important qualitative information can be gained from the present data. In Figs. 1(b) and 1(d) the positions of the AMRO features around ±53° are remarkably similar for $x = 0.16$ and 0.17. Moreover, as illustrated in Fig. 2 they exhibit the same dependence on the azimuthal angle φ of the field direction. This means that the cyclotron orbits responsible for the AMRO are identical for these two doping levels. At first glance, this conclusion contradicts the SdH data [5] which exhibit a dramatic change in the oscillation spectrum when moving from $x = 0.16$ to 0.17. The apparent discrepancy can be resolved by taking into account the possibility of magnetic breakdown between the holelike and electronlike parts of the reconstructed Fermi surface.

The characteristic breakdown field B_0 can be estimated using the Blount criterion [21], $\hbar\omega_0 \sim \Delta^2/\varepsilon_F$, where $\omega_0 = eB_0/m_c$, e is the elementary charge, m_c the cyclotron mass corresponding to the orbit on the original large Fermi cylinder, ε_F the Fermi energy, and Δ the energy gap between the holelike and electronlike bands determined by the density-wave potential. Using $\Delta \simeq 30$ meV [5], $m_c \approx 2 \times 10^{-30}$ kg (estimated from the T dependence of the amplitude of the fast SdH oscillations in the $x = 0.17$ sample), and $\varepsilon_F \simeq 0.5$ eV, we obtain $B_0 \sim 35$ T. Although this is a rather rough estimate, it clearly shows that magnetic

breakdown can indeed be expected for overdoped NCCO crystals within the experimentally available field range.

If the magnetic breakdown scenario applies to our samples, the cyclotron orbit topology becomes dependent on the magnetic field strength. In particular, for $B \sim B_0$ both the small classical orbits on the reconstructed Fermi surface and the large orbit, indistinguishable from that on the original Fermi surface, can be realized. To check this, we have carried out refined measurements of the SdH oscillations in strongly overdoped NCCO in pulsed magnetic fields. Figure 3 shows examples of the SdH oscillations in the interlayer resistance of an $x = 0.17$ crystal at $T \approx 2.5$ and 5.6 K [22]. Two oscillation frequencies are readily resolved at both temperatures. Fast oscillations with frequency $F_{\text{fast}} = 10.93 \pm 0.05$ kT, consistent with our previous report [5], are observed starting from ≈ 55 T. They are superimposed by slow oscillations which can be traced down to below 40 T. Their frequency, $F_{\text{slow}} = 250 \pm 10$ T, is similar to the values obtained for crystals with $x = 0.15$ and 0.16 and attributed to small hole pockets of the reconstructed Fermi surface.

One has to beware of sample inhomogeneity as a possible source of coexisting SdH frequencies. Evidently, a minor volume fraction with $x \approx 0.16$ might produce weak slow oscillations in addition to the fast ones originating from the $x = 0.17$ matrix. Therefore, we did a careful sample characterization including x-ray and magnetization studies, assuring a high crystal quality and doping homogeneity within ±0.25%. However, the strongest argument regarding the origin of the slow oscillations is provided by the doping dependence of their frequency shown by Fig. 4. Were the oscillations caused by a small volume fraction

FIG. 3 (color online).   Slow and fast SdH oscillations in the interlayer resistance of a strongly overdoped, $x = 0.17$, NCCO crystal recorded at two different temperatures. The data are normalized to the field-dependent nonoscillating background resistance. The inset shows high-field fragments of the data, demonstrating regular fast oscillations.
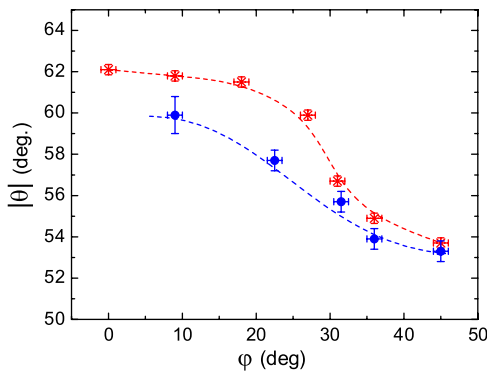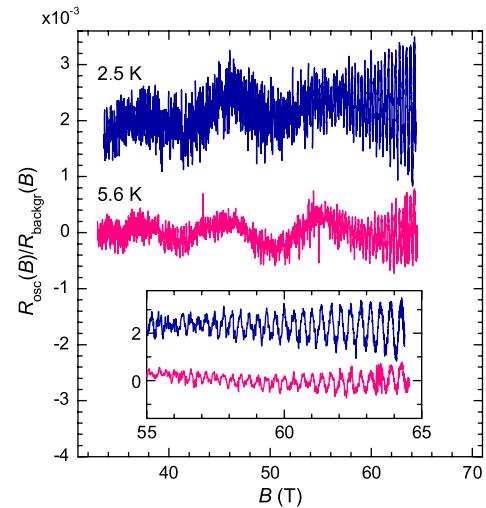

FIG. 2 (color online).   Dependence of the positions of the AMRO features in NCCO with $x = 0.16$ (blue circles) and 0.17 (red stars) on the azimuthal orientation φ of the field rotation plane. Dashed lines are guides to the eye.
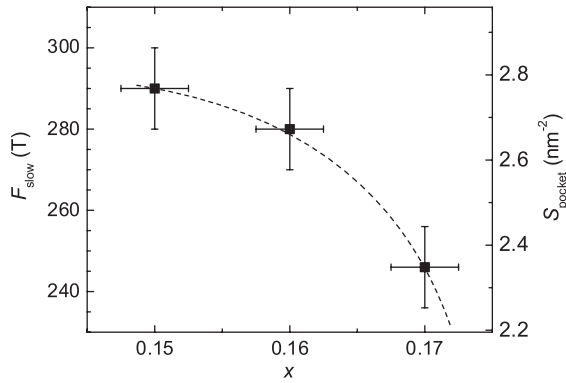
FIG. 4.   Frequency of the slow SdH oscillations (left scale) and the corresponding Fermi surface area (right scale) as a function of the electron doping level x. The dashed line is a guide to the eye.

with a lower doping level, a change of the nominal Ce concentration x would affect their amplitude but not the frequency. By contrast, the experiment shows a clear decrease of F_{slow} with increasing x. This is fully consistent with the expected decrease in the size of the small hole pockets of the reconstructed Fermi surface at increasing the electron doping.

Thus, we conclude that the slow SdH oscillations are intrinsic to NCCO with $x = 0.17$. They clearly indicate that the Fermi surface is still reconstructed even at this doping level, the highest attainable in a bulk NCCO crystal [20]. The corresponding superlattice potential is, however, very weak, allowing for magnetic breakdown as evidenced by the observation of the fast SdH oscillations.

As noted earlier [5], the presence of a superstructure in the electronic system of overdoped NCCO seems to contradict neutron scattering [23] and ARPES [7,8] results. One possibility to resolve this apparent disagreement is to consider a hidden d-density wave ordering [24]. On the other hand, it may be that the ordering exists at high magnetic fields, i.e., at the conditions of our present experiment. While there are some evidences supporting this scenario [25,26], the question is far from being settled [27]. To this end, it would be highly desirable to perform magnetic spectroscopy experiments on high-quality overdoped NCCO crystals showing magnetic quantum oscillations.

*Mark.Kartsovnik@wmi.badw-muenchen.de

[1] N. Doiron-Leyraud, C. Proust, D. LeBoeuf, J. Levallois, J.-B. Bonnemaison, R. Liang, D. A. Bonn, W. N. Hardy, and L. Taillefer, Nature (London) **447**, 565 (2007).

[2] E. A. Yelland, J. Singleton, C. H. Mielke, N. Harrison, F. F. Balakirev, B. Dabrowski, and J. R. Cooper, Phys. Rev. Lett. **100**, 047003 (2008).

[3] A. F. Bangura et al., Phys. Rev. Lett. **100**, 047004 (2008).

[4] B. Vignolle, A. Carrington, R. A. Cooper, M. M. J. French, A. P. Mackenzie, C. Jaudet, D. Vignolles, C. Proust, and N. E. Hussey, Nature (London) **455**, 952 (2008).

[5] T. Helm, M. V. Kartsovnik, M. Bartkowiak, N. Bittner, M. Lambacher, A. Erb, J. Wosnitza, and R. Gross, Phys. Rev. Lett. **103**, 157002 (2009).

[6] S. Massidda, N. Hamada, J. Yu, and A. J. Freeman, Physica (Amsterdam) **157C**, 571 (1989).

[7] N. P. Armitage et al., Phys. Rev. Lett. **88**, 257001 (2002).

[8] H. Matsui, T. Takahashi, T. Sato, K. Terashima, H. Ding, T. Uefuji, and K. Yamada, Phys. Rev. B **75**, 224514 (2007).

[9] Y. Dagan, M. M. Qazilbash, C. P. Hill, V. N. Kulkarni, and R. L. Greene, Phys. Rev. Lett. **92**, 167001 (2004).

[10] M. Lambacher, Ph.D. thesis, Technische Universität München, 2008.

[11] J. Eun, X. Jia, and S. Chakravarty, Phys. Rev. B **82**, 094515 (2010).

[12] M. V. Kartsovnik, Chem. Rev. **104**, 5737 (2004).

[13] C. Bergemann, A. P. Mackenzie, S. R. Julian, D. Forsythe, and E. Ohmichi, Adv. Phys. **52**, 639 (2003).

[14] M. Baxendale, V. Z. Mordkovich, and S. Yoshimura, Solid State Commun. **107**, 165 (1998).

[15] K. Yamaji, J. Phys. Soc. Jpn. **58**, 1520 (1989).

[16] M. V. Kartsovnik, V. N. Laukhin, S. I. Pesotskii, I. F. Schegolev, and V. M. Yakovenko, J. Phys. I (France) **2**, 89 (1992).

[17] N. E. Hussey, M. Abdel-Jawad, A. Carrington, A. P. Mackenzie, and L. Balicas, Nature (London) **425**, 814 (2003).

[18] P. D. Grigoriev, Phys. Rev. B **81**, 205122 (2010).

[19] M. Abdel-Jawad, M. P. Kennet, L. Balicas, A. Carrington, A. P. Mackenzie, R. H. McKenzie, and N. E. Hussey, Nature Phys. **2**, 821 (2006).

[20] M. Lambacher, T. Helm, M. Kartsovnik, and A. Erb, Eur. Phys. J. Special Topics **188**, 61 (2010).

[21] D. Shoenberg, Magnetic Oscillations in Metals (Cambridge University Press, Cambridge, England, 1984).

[22] Overheating of the sample due to the applied transport current, $I = 5$–10 mA, and fast field sweep rate was not negligible. Therefore, the sample temperature was estimated by comparing the superconducting transition in the $R(B)$ curves with those recorded at small currents, $I = 10$–100 μA, in a steady magnetic field.

[23] E. M. Motoyama, G. Yu, I. M. Vishik, O. P. Vajk, P. K. Mang, and M. Greven, Nature (London) **445**, 186 (2007).

[24] S. Chakravarty, R. B. Laughlin, D. K. Morr, and C. Nayak, Phys. Rev. B **63**, 094503 (2001); X. Jia, P. Goswami, and S. Chakravarty, Phys. Rev. B **80**, 134503 (2009).

[25] M. Matsuura, P. Dai, H. J. Kang, J. W. Lynn, D. N. Argyriou, K. Prokes, Y. Onose, and Y. Tokura, Phys. Rev. B **68**, 144503 (2003).

[26] J. E. Sonier, K. F. Poon, G. M. Luke, P. Kyriakou, R. I. Miller, R. Liang, C. R. Wiebe, P. Fournier, and R. L. Greene, Phys. Rev. Lett. **91**, 147002 (2003).

[27] N. P. Armitage, P. Fournier, and R. L. Greene, Rev. Mod. Phys. **82**, 2421 (2010).